FIB-SEM investigation of trapped intermetallic particles in anodic oxide films on AA1050 aluminium

M. Jariyaboon
Department of Mechanical Engineering, Technical University of Denmark, Lyngby, Denmark
Department of Chemistry, Faculty of Science, Mahidol University, Bangkok, Thailand and
Center for Surface Science and Engineering, Faculty of Science, Mahidol University, Salaya, Thailand

P. Møller
Department of Mechanical Engineering, Technical University of Denmark, Lyngby, Denmark

R.E. Dunin-Borkowski
Center for Electron Nanoscopy, Technical University of Denmark, Lyngby, Denmark, and

R. Ambat
Department of Mechanical Engineering, Technical University of Denmark, Lyngby, Denmark

Abstract

Purpose – The purpose of this investigation is to understand the structure of trapped intermetallics particles and localized composition changes in the anodized anodic oxide film on AA1050 aluminium substrates.

Design/methodology/approach – The morphology and composition of Fe-containing intermetallic particles incorporated into the anodic oxide films on industrially pure aluminium (AA1050, 99.5 per cent) has been investigated. AA1050 aluminium was anodized in a 100 ml/l sulphuric acid bath with an applied voltage of 14 V at 20°C ± 2°C for 10 or 120 min. The anodic film subsequently was analyzed using focused ion beam-scanning electron microscopy (FIB-SEM), SEM, and EDX.

Findings – The intermetallic particles in the substrate material consisted of Fe or both Fe and Si with two different structures: irregular and round shaped. FIB-SEM cross-sectioned images revealed that the irregular-shaped particles were embedded in the anodic oxide film as a thin strip structure and located near the top surface of the film, whereas the round-shaped particles were trapped in the film with a spherical structure, but partially dissolved and were located throughout the thickness of the anodic film. The Fe/Si ratio of the intermetallic particles decreased after anodizing.

Originality/value – This paper shows that dual beam FIB-SEM seems to be an easy, less time consuming and useful method to characterize the cross-sectioned intermetallic particles incorporated in anodic film on aluminium.

Keywords Anodic protection, Anodizing, AA1050, Intermetallic particle, FIB-SEM, Oxides, Organometallic compounds

Paper type Research paper

1. Introduction

Anodizing has been used widely in the surface treatment of aluminium and its alloys for applications in the aerospace, architectural, and automotive industries. The anodic oxide films formed during anodizing can improve significantly the performance of the substrates by increasing corrosion resistance, increasing surface hardness, colouring, improving lubrication, and improving adhesion behaviour.

There have been a number of reports (Dasquet *et al.*, 2000; Fratila-Apachitei *et al.*, 2004a, b; Habazaki *et al.*, 2001; Mukhopadhyay and Sharma, 1997; Páez *et al.*, 1996; Shimizu *et al.*, 2000, 1998, 1997; Tsangaraki-Kaplanoglou *et al.*, 2006; Zhou *et al.*, 1997; Zhuravlyova *et al.*, 2002) showing that the presence of second-phase particles in the aluminium alloys substrates influences the anodic oxide films. They modify the composition and growth of film as well as microstructure during anodizing. In addition, the second-phase particles incorporated into the anodic films affect the pore morphology, create cracks and voids, and affect oxygen evolution (Páez *et al.*, 1996; Shimizu *et al.*, 1997; Zhou *et al.*, 1997; Zhuravlyova *et al.*, 2002). The quality of anodic oxide films depends on amount, type, and distribution of the second-phase particles, which exhibit different dissolution behaviour during anodizing compared to aluminium matrix (Fratila-Apachitei *et al.*, 2004a; Mukhopadhyay and Sharma, 1997).

The current issue and full text archive of this journal is available at **www.emeraldinsight.com/0003-5599.htm**

Anti-Corrosion Methods and Materials
58/4 (2011) 173–178

[DOI 10.1108/00035591111148885]

M. Jariyaboon is supported by The Hans Christian Ørsted Postdoc Fellowship Programme. The authors would like to thank A. Nicole MacDonald (Center for Electron Nanoscopy, Technical University of Denmark) for her assistance in FIB-SEM.

Thus, the understanding of structure and distribution of second-phase particles incorporated into the anodic oxide films is greatly important in determining properties of the anodic films. In the present investigation, the structure of Fe-containing intermetallic particles incorporated into the anodic oxide films on industrially pure aluminium (AA1050) has been investigated. The AA1050 was anodized in sulphuric acid at 14 V. The cross-sections of intermetallic particles incorporated into the film as well as cross-sections of the anodized layer were analyzed using focused ion beam-scanning electron microscopy (FIB-SEM), SEM, and EDX.

2. Experimental

2.1 Material

The material used in this work was an industrially pure AA1050 (99.5 wt%) aluminium in the form of sheet. All specimens were cut from the sheet with dimensions of $30 \times 20 \times 1$ mm and were then ground and polished to 1 μm diamond finish prior to the anodizing process.

2.2 Pre-treatment and anodizing process

Before anodizing, the specimens were pre-treated as follows: cleaning with 60 g/l Alficlean 136 at 60°C $\pm$4°C for 4 min, rinsing with deionized water for 2 min, immersing in 55 ml/l HNO_3 at room temperature for 2 min and then rinsing with deionized water for 2 min.

The anodizing process was carried out in 100 ml/l H_2SO_4 at 20°C $\pm$2°C with a constant applied potential of 14 V for 10 min or 120 min. After anodizing, the specimens were rinsed thoroughly with deionized water for 1 min and air dried.

2.3 Microscopic investigation

Microstructural and chemical analysis of the pre-treated and anodized AA1050 aluminium on the top surface and cross-section was performed by scanning electron microscopy (SEM) (JEOL 5900) linked with EDX and dual beam FIB-SEM (FEI Quanta 3D).

The dual beam FIB-SEM was used for cross-section milling of the intermetallic particles incorporated into the anodic films after anodizing for 10 min. The cross-section milling was performed at a tilting angle of 52°. A Ga ion beam was operated at 30 kV with a current in a range of 0.5-20 nA. Before milling, the intermetallic particles were deposited by Pt with a thickness of 1 μm in order to protect the areas of interest from the damage caused during milling.

3. Results

3.1 Microstructure of AA1050 after pre-treatment

The SEM image (SE mode) of AA1050 after pre-treatment is shown in Figure 1. There are two types of constituent intermetallic particles: irregular-shaped and round-shaped particles. The density of the irregular-shaped particles was higher than was that of the round-shaped particles, as shown in Figure 1(a). The higher magnification images of irregular-shaped and round-shaped particles are shown in Figure 1(b) and (c), respectively. It is evident that the round-shaped particles were partially dissolved during the pre-treatment process. It should be noted that for as received AA1050, the round-shaped particles are not solid and are small particles loosely packed together.

Figure 1 SEM images of AA1050 after pre-treatment process

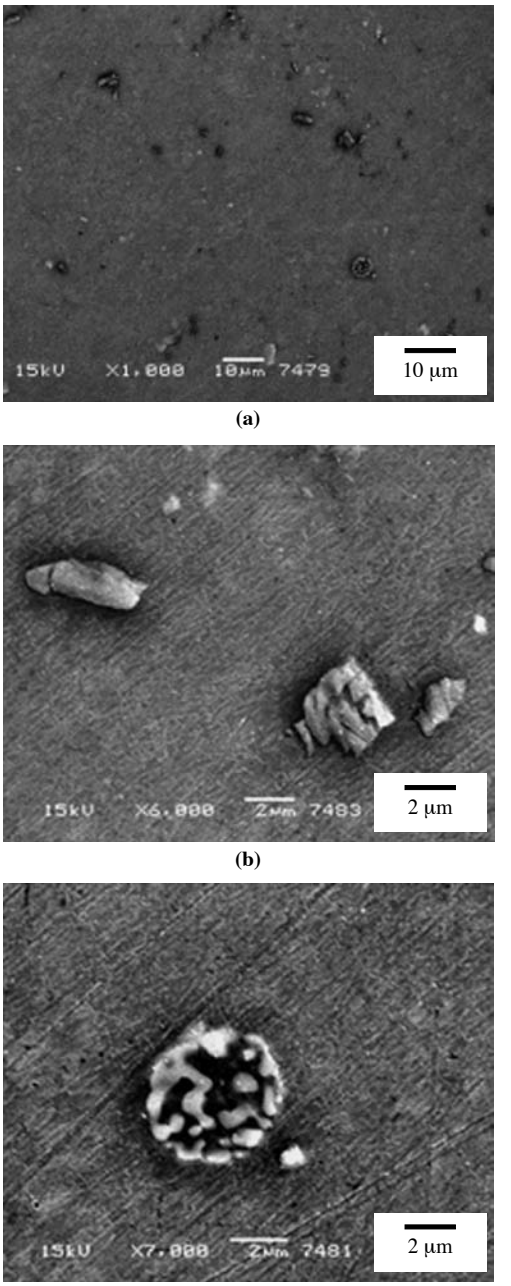

Notes: (a) General view at low magnification; (b) irregular-shape; (c) roundshape Fe-containing particles at high magnification

EDX analysis showed that the constituents of intermetallic particles in AA1050 consist of Fe or both Fe and Si. It is likely that the round-shaped particles contain more Si, compared with the irregular-shaped particles.

3.2 Microstructure of AA1050 after anodizing in H_2SO_4 for 10 min

Figures 2(a) and 3(a) show the SEM images (SE mode) of the irregular-shaped and round-shaped Fe-containing particles after anodizing in 100 ml/l H_2SO_4 at 14 V for 10 min, respectively.

Figure 2 SEM images of AA1050 after anodizing for 10 min

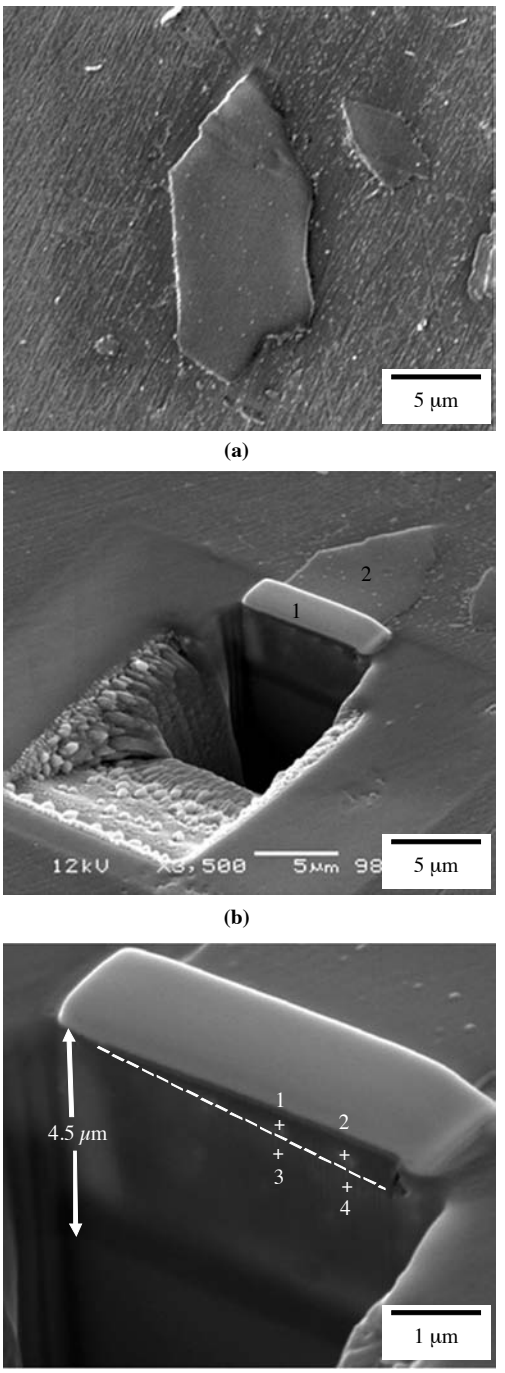

Notes: (a) Irregular-shape Fe-containing particle embedded in anodic oxide film; (b) low magnification; (c) high-magnification cross-sectioned SEM images of the particle shown in (a); numbers are given as references for EDX analysis

Figure 3 SEM images of AA1050 after anodizing for 10 min

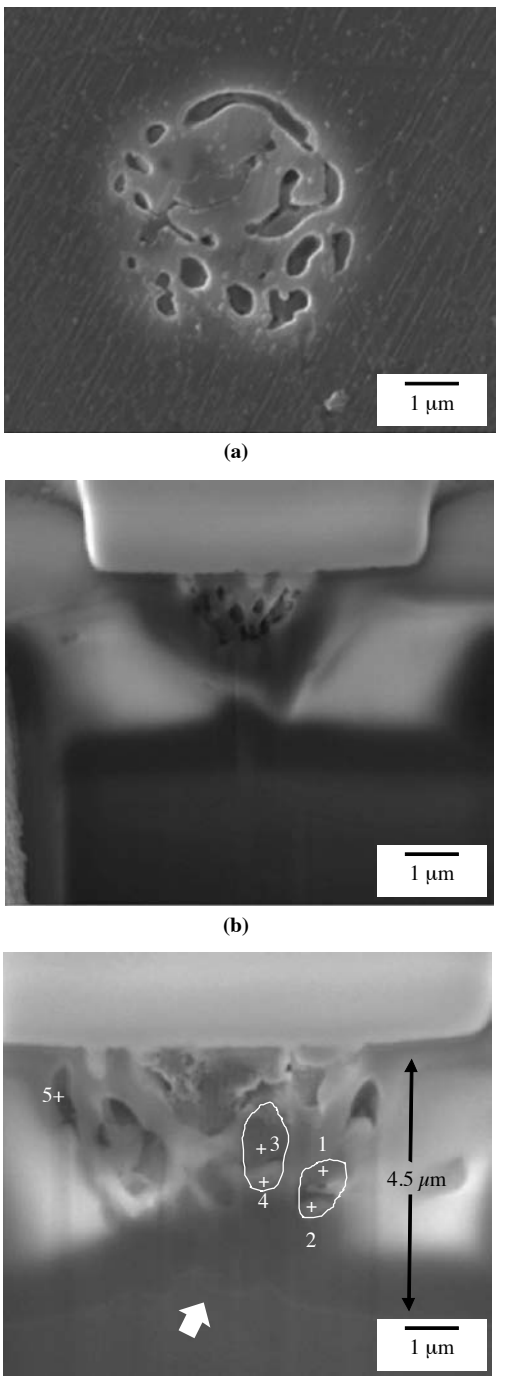

Notes: (a) Round-shape Fe-containing particle embedded in anodic oxide film; (b) cross-sectioned SEM image near the edge of particle; (c) near the middle of the particle shown in (a); numbers are given as references for EDX analysis

It is clearly seen that both types of Fe-containing particles still remain in the anodized layer and the thickness of anodic oxide film is approximately 4.5 μm, as seen in Figures 2(c) and 3(c).

Figure 2(b) shows an example of an SEM image at low magnification after cross-section milling, using the FIB-SEM. The cross-section milling was performed to the mid-section of the intermetallic particle shown in Figure 2(a). Number 1 is the

area where Pt was deposited on the intermetallic particle before cross-section milling in order to protect the intermetallic particle from damage during the milling process. Number 2 is the area of the remaining intermetallic particle.

Figure 2(c) shows the cross-section SEM image at higher magnification of the irregular-shaped Fe-containing intermetallic particle. It can be seen that the particle is embedded in the anodic oxide film and it is located near the top of the anodic oxide film with a thin strip structure (above the white dotted line).

The EDX analysis at different points defined in Figure 2(c) is shown in Table I. It confirms that there was no Fe below the white dashed line. O and S could be found in the particles. The presence of Ga and Pt is due to the contamination from Ga ion beam and Pt deposition.

Figure 3(b) and (c) show the cross-sectioned SEM images of the round-shaped Fe-containing intermetallic particle, near the edge and near the middle of the particle, respectively. As shown in Figure 3(c), the particles were incorporated into the anodic oxide film and were distributed throughout the thickness of the anodic oxide film. The particle shows a spherical structure associated with partial dissolution. It should be noted that the substructure of the particle, as indicated by the white solid line, consists of a brighter part at the bottom and a darker part at the top. A scalloped structure also can be observed below the particle at the interface between the anodic oxide film and the aluminium substrate as indicated by an arrow.

The EDX analysis of each area of the particle shown in Figure 3(c) is given in Table II. It is clearly evident that the brighter part contains more Fe and Si but less O, as compared to the darker part (compare positions 1 and 2, and 3 and 4). For EDX analysis at area 5, Fe and Si cannot be found, indicating a void in the structure. Ga and Pt can also be observed due to contamination during the milling process.

3.3 Microstructure of AA1050 after anodizing in H_2SO_4 for 120 min

The cross-sectioned SEM image (BSE mode) of the anodized layer of AA1050, after anodizing in H_2SO_4 for 120 min, is shown in Figure 4. The thickness of the anodic oxide layer was approximately 35 μm.

Figure 4(a) and (b) show the microstructure at the interface between the anodic oxide film and the aluminium substrate, with round-shaped and irregular-shaped Fe-containing particles. Both types of particles show a similar behaviour. The lower part of particle located in the aluminium was brighter, whereas the upper part of particle located in the anodic oxide layer appeared darker. The upper part of particle protruded into the film grown over the particle and surrounding matrix regions.

Table I EDX analysis of cross-sectioned AA1050 of the irregular-shape particle after anodizing for 10 min

	Element (wt%)						
No.	O	Al	Si	S	Fe	Ga	Pt
1	14.12	60.50	–	9.25	3.47	2.54	10.11
2	13.12	58.27	0.91	9.76	6.36	2.27	9.29
3	17.46	69.75	–	11.04	–	2.15	–
4	17.26	70.03	–	10.87	–	1.85	–

Note: Reference numbers are defined in Figure 2(c)

Table II EDX analysis of cross-sectioned AA1050 of the round-shape particle after anodizing for 10 min

	Element (wt%)						
No.	O	Al	Si	S	Fe	Ga	Pt
1	12.41	62.02	4.68	8.53	7.15	2.21	–
2	7.39	61.89	6.89	5.75	16.14	2.58	–
3	10.34	57.01	3.65	7.58	5.67	2.69	13.05
4	7.85	62.71	5.06	5.52	16.54	2.32	–
5	13.34	67.64	–	11.27	–	1.84	5.91

Note: Reference numbers are defined in Figure 3(c)

The EDX analysis illustrated in Table III shows that the Fe content in the upper part of the particles embedded in the anodic oxide film was less than that of the remaining particles in the aluminium, and the Fe/Si ratio was lower when the particles were in the anodic oxide film (compare positions 1 and 2 in Figure 4(a), 3 and 4 in Figure 4(b)). O could be detected in the part of particles incorporated into the anodic oxide film.

It can be noticed that the Fe-containing particles survive and remain in the anodic oxide film after anodizing for 120 min as shown in Figure 4(c). The brighter part of the particles, which contained more Fe than that of the darker part, could still be found (compare positions 5 and 6). In addition to some voids, the dark grey coloured particle indicated as position 7 in Figure 4(c) is observed. This type of particle contained only Si.

4. Discussion

The presence of Fe-containing, Si-containing or Fe-Si-containing particles in AA1050 aluminium influences the local morphology and composition of the anodic oxide layer.

Work done by Fratila-Apachitei *et al.* (2004a, b) has shown that the Al-Fe, Al-Fe-Si, and Al-Si particles anodize at a lower rate than does the aluminium matrix, causing the incorporation of the particles into the anodized layer as well as creating a locally scalloped structure underneath the particles. Tortuous porosity also is observed around the Si particles.

Mukhopadhyay and Sharma (1997) studied the effect of Fe-containing particles on the anodized AA7075. The morphology and distribution of $Al_{12}(FeMn)_3Si$ particles influence the quality of the anodic film. The $Al_{12}(FeMn)_3Si$ particles in AA7075 locally impair anodic film growth and constrain the film to grow by bypassing them leading to the discontinuous anodized layers. A greater impact occurs when the orientation of particles is normal to the anodic film growth direction. The degree of continuity of the anodic oxide film depends on the density of $Al_{12}(FeMn)_3Si$ particles. A larger number of $Al_{12}(FeMn)_3Si$ particles leads to more discontinuity in the film and the larger the size of the particles then the more gaps are created in the anodic film.

The studies of the effect of Fe-containing particles on the anodic oxide layer of Al-0.5Fe and Al-1.4Fe alloys by Shimizu *et al.*, 1998 have shown that compositions of Fe-containing particles significantly affect the anodized layer. The Al_6Fe particles are partially oxidized as well as incorporated into the anodized layer, while the Al_3Fe particles cannot be observed in the anodized layer as they are oxidised at the same rate as the aluminium matrix.

The results of the present work clearly show that both types (round and irregular shape) of the Fe-containing particles are

Figure 4 SEM images (BSE mode) of AA1050 after anodizing for 120 min showing interface between the anodic oxide film/aluminium substrate of (a) round-shape, (b) irregular-shape Fe-containing particles, and (c) Fe-containing particles embedded in the anodic oxide film

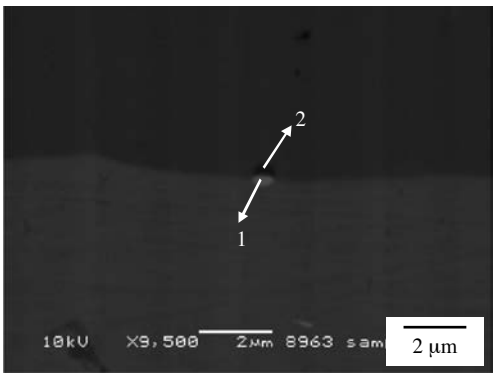

(a)

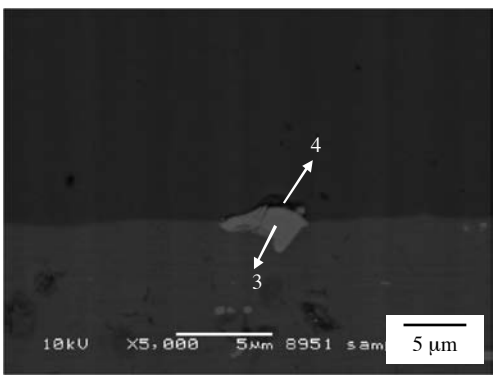

(b)

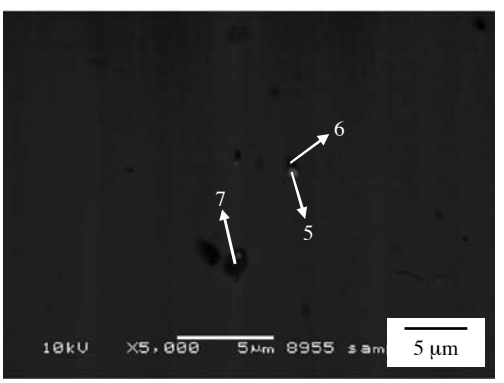

(c)

Note: Numbers are given as references for EDX analysis

incorporated into the anodic oxide film as a result of a lower oxidation rate compared with the aluminium matrix (Fratila-Apachitei *et al.*, 2004a, b; Shimizu *et al.*, 1998). However, the structure of each type of the particles trapped into the anodic oxide film is different.

The irregular-shaped particle, which consists of less Si or no Si, is embedded only near the top of anodic oxide film with a thin strip structure, whereas the round-shaped particle, which contains more Si, is partially dissolved and embedded with a spherical structure. The local scalloped structure at the interface between the anodic oxide film/aluminium can be observed only for the round-shaped particle (see arrow in Figure 3(c)). The presence of the scalloped structure indicates a lower rate of oxidation compared to the aluminium matrix (Fratila-Apachitei *et al.*, 2004b). This implies that the irregular-shape Fe-containing particle undergoes oxidation at a higher rate than that of the round-shaped Fe-containing particle. It is suspected that this is due to the presence of Si, which is likely to be stable in an acidic bath.

Table III EDX analysis of cross-sectioned AA1050 after anodizing for 120 min

	Element (wt%)					
No.	O	Al	Si	S	Fe	Fe/Si
1	–	85.18	3.10	–	11.72	3.78
2	8.17	67.68	18.02	6.13	–	0.00
3	–	67.87	7.00	–	25.13	3.59
4	8.51	72.26	3.99	8.85	6.39	1.60
5	6.10	72.99	2.08	4.53	14.29	6.87
6	11.04	64.15	15.23	9.59	–	0.00
7	9.89	69.21	11.23	8.67	–	0.00

Note: Reference numbers are defined in Figure 4

As seen in Figure 3(c), the round-shaped Fe-containing particle undergoes partial dissolution and partial oxidation. It should be noted that some partial dissolution occurs during the pre-treatment process. The upper (darker) part of the substructure, as defined by the solid white line, is likely to dissolve and oxidize with a higher rate than that of the lower (brighter) part, as shown from the EDX results (Table II).

After anodizing for 120 min, voids, particles containing Si, or particle containing both Fe and Si are observed in the anodized layer. It is evident that the ratio between Fe/Si becomes lower after anodizing. This implies that Fe dissolves at a faster rate than Si. In addition, oxygen is also found in Si-containing and Fe-Si-containing particles, possibly indicating partial oxidation (Fratila-Apachitei *et al.*, 2004b; Habazaki *et al.*, 2001).

5. Conclusions

FIB-SEM microscopy of the two types of Fe-containing particles trapped in the anodic oxide film developed on AA1050 has shown clearly that the structure of each type is different in the anodic oxide film. The irregular-shaped particles show a thin strip structure in the anodized layer, whereas the round-shaped particles show a spherical structure with partial dissolution.

The Fe-containing particles in AA1050 show a lower anodic oxidation rate compared to the aluminium matrix. A change in the composition of the Fe-containing particles is also observed after anodizing, such that the ratio of Fe/Si becomes lower.

References

Dasquet, J.-P., Caillard, D., Conforto, E., Bonino, J.-P. and Bes, R. (2000), "Investigation of the anodic oxide layer on 1050 and 2024T3 aluminium alloys by electron microscopy and electrochemical impedance spectroscopy", *Thin Solid Films*, Vol. 371 Nos 1/2, pp. 183-90.

Fratila-Apachitei, L.E., Terryn, H., Skeldon, P., Thompson, G.E., Duszczyk, J. and Katgerman, L. (2004a), "Influence

of substrate microstructure on the growth of anodic oxide layers", *Electrochimica Acta*, Vol. 49 No. 7, pp. 1127-40.

Fratila-Apachitei, L.E., Tichelaar, F.D., Thompson, G.E., Terryn, H., Skeldon, P., Duszczyk, J. and Katgerman, L. (2004b), "A transmission electron microscopy study of hard anodic oxide layers on AlSi(Cu) alloys", *Electrochimica Acta*, Vol. 49 No. 19, pp. 3169-77.

Habazaki, H., Shimizu, K., Skeldon, P., Thompson, G.E. and Wood, G.C. (2001), "The behaviour of iron during anodic oxidation of sputtering-deposited Al-Fe alloys", *Corrosion Science*, Vol. 43 No. 7, pp. 1393-402.

Mukhopadhyay, A.K. and Sharma, A.K. (1997), "Influence of Fe-bearing particles and nature of electrolyte on the hard anodizing behavior of AA7075 extrusion products", *Surface and Coatings Technology*, Vol. 92 No. 3, pp. 212-20.

Páez, M.A., Foong, T.M., Ni, C.T., Thompson, G.E., Shimizu, K., Habazaki, H., Skeldon, P. and Wood, G.C. (1996), "Barrier-type anodic film formation on an Al-3.5 wt% Cu alloy", *Corrosion Science*, Vol. 38 No. 1, pp. 59-72.

Shimizu, K., Kobayashi, K., Thompson, G.E., Skeldon, P. and Wood, G.C. (1997), "The influence of θ' precipitates on the anodizing behaviour of binary Al-Cu alloys", *Corrosion Science*, Vol. 39 No. 2, pp. 281-4.

Shimizu, K., Brown, G.M., Kobayashi, K., Skeldon, P., Thompson, G.E. and Wood, G.C. (1998), "Ultramicrotomy-a route towards the enhanced understanding of the corrosion and filming behaviour of aluminium and its alloys", *Corrosion Science*, Vol. 40 No. 7, pp. 1049-72.

Shimizu, K., Brown, G.M., Habazaki, H., Kobayashi, K., Skeldon, P., Thompson, G.E. and Wood, G.C. (2000), "Selective oxidation of aluminium and interfacial enrichment of iron during anodic oxide growth on an Al_6Fe phase", *Corrosion. Science*, Vol. 42 No. 5, pp. 831-40.

Tsangaraki-Kaplanoglou, T., Theohari, S., Dimogerontakis, Th., Wang, Y.-M., Kuo, H.-H. and Kia, S. (2006), "Effect of alloy types on the anodizing process of aluminum", *Surface and Coatings Technology*, Vol. 200 No. 8, pp. 2634-41.

Zhou, X., Thompson, G.E., Habazaki, H., Shimizu, H., Skeldon, P. and Wood, G.C. (1997), "Copper enrichment in Al-Cu alloys due to electropolishing and anodic oxidation", *Thin Solid Films*, Vol. 293 Nos 1/2, pp. 327-32.

Zhuravlyova, E., Iglesias-Rubianes, L., Pakes, A., Skeldon, P., Thompson, G.E., Zhou, X., Quance, T., Graham, M.J., Habazaki, H. and Shimizu, K. (2002), "Oxygen evolution within barrier oxide films", *Corrosion Science*, Vol. 44 No. 9, pp. 2153-9.

Corresponding author

R. Ambat can be contacted at: ram@mek.dtu.dk